Contribution of the epididymis beyond fertilization: relevance of CRISP1 and CRISP3 for sperm DNA integrity and early embryo development

Sulzyk Valeria; Curci Ludmila; González Lucas N; Rebagliati Cid Abril; Weigel Muñoz Mariana*; Cuasnicu Patricia S[&]*.

Instituto de Biología y Medicina Experimental (IByME-CONICET), Buenos Aires, C1428ADN, Argentina.

[&] Corresponding author: pcuasnicu@gmail.com; Vuelta de Obligado 2490, Buenos Aires, Argentina

* These authors have contributed equally to this work and share last authorship

Abstract

Numerous reports show that the epididymis plays a key role in the acquisition of sperm fertilizing ability but less information exists on its contribution to embryo development. Evidence from our laboratory showed that mammalian CRISP (Cysteine-Rich Secretory Proteins), known to be expressed in the epididymis, to regulate calcium (Ca^{2+}) channels and to participate in fertilization, may also be relevant for embryo development. More specifically, we found that males with simultaneous mutations in *Crisp1* and *Crisp3* genes exhibited normal *in vivo* fertilization but impaired embryo development. In the present work, aimed to investigate the mechanisms underlying this reproductive phenotype, we observed that embryo development failure was not due to delayed fertilization as no differences in sperm transport within the female tract nor in *in vivo* fertilization were found shortly after mating. The observation that impaired embryo development was also found in eggs fertilized by epididymal sperm either after uterine insemination or *in vitro* fertilization, revealed that the defects were already present at epididymal level. Of note, eggs fertilized *in vitro* by mutant sperm exhibited impaired meiotic resumption not due to defects in Ca^{2+}oscillations during egg activation, prompting us to examine potential sperm DNA defects. Interestingly, DNA fragmentation was found in cauda but not caput epididymal mutant sperm revealing that DNA integrity defects appear during epididymal maturation. Moreover, exposure of control sperm to mutant epididymal fluid significantly increased DNA fragmentation, indicating the relevance of the luminal environment for sperm DNA integrity. The finding that incubation of sperm with control epididymal fluid in the presence of Ca^{2+} also increased DNA fragmentation together with the higher intracellular Ca^{2+} levels detected in mutant sperm supports a dysregulation of Ca^{2+} homeostasis as the main responsible for DNA fragmentation and subsequent early development failure of mutant males. Together, our results support the contribution of the epididymis beyond fertilization, identifying CRISP1 and CRISP3 as novel male factors relevant for DNA integrity and early embryo development. Given the existence of human functional homologues of CRISP and the incidence of DNA fragmentation in infertile men, we believe these findings not only provide relevant information on the impact of epididymal factors on embryonic development but will also contribute to a better understanding, diagnosis and treatment of human infertility.

Introduction

Mammalian sperm that leave the testes do not have the ability to fertilize an egg and must undergo different processes to become fertilizing competent. Initially, they need to mature while they pass through the epididymis which provides a suitable environment for acquisition of fertilizing ability, storage and protection of sperm (Robaire *et al.*, 2015). Subsequently, sperm must undergo another process known as capacitation while ascending through the female reproductive tract which will allow them to undergo the acrosome reaction in the head and to develop a hyperactivated motility in the tail, both essential for fertilization (Florman *et al.*, 2015). Once they reach the site of fertilization in the oviduct, sperm penetrate the different coats that surround the egg (i.e. cumulus oophorus and zona pellucida (ZP)) and fuse with the plasma membrane of the egg, resulting in the formation of a single-cell zygote which then embarks on its development into a multicellular organism through a highly complex and tightly regulated process (Ramathal *et al.*, 2015). Whereas numerous reports show the relevance of post-testicular maturation for fertilization, less information exists on the contribution of epididymal transit to embryo development.

The epididymis, the main location where sperm maturation takes place, has a very specialized epithelium involved in ion transport, protein matrix formation, and both protein and vesicle secretion (Robaire *et al.,* 2015). Among such secretory proteins are CRISP (Cysteine-RIch Secretory Proteins), a group of evolutionarily conserved proteins mainly expressed in the male reproductive tract (Gibbs et al, 2008; Gonzalez *et al.*, 2021). In mammals, four members have been described which escort sperm during their transit through both the male and female reproductive tracts. CRISP are characterized by the presence of 16 conserved Cys and two domains that have evolved to perform a variety of functions. Whereas the N-terminal domain of CRISP proteins (i.e. PR-1) is involved in cell to cell interaction (Ellerman *et al*., 2006; Maeda *et al.*, 1998), proteolytic processes (Milne *et al*., 2003) and amyloid-like-aggregation activity (Olrichs *et al*., 2014, Sheng *et al*., 2019), the C-terminal domain (i.e. CRD) has the ability to regulate ion channels, such as ryanodine (RyR), CNGs, TRPM8 and Catsper (Ernesto *et al*., 2015; Gibbs *et al.,* 2006; Gibbs *et al.*, 2011; Yamazaki *et al.*, 2002).

Biochemical, molecular and genetic approaches from our group and others revealed that CRISP proteins play key roles in sperm maturation, capacitation and fertilization (Gonzalez *et al*., 2021). Epididymal CRISP1, first described by our laboratory (Cameo and Blaquier, 1976), (Cohen *et al.,* 2000a) associates with sperm during maturation and both inhibits CatSper (Ernesto *et al.,* 2015), the primary sperm Ca^{2+} channel essential for male fertility (Ren *et al.,* 2001; Sun *et al.*, 2017), and participates in gamete interaction through egg-complementary sites (Busso *et al.,* 2007; Cohen *et al.*, 2000b; Rochwerger *et al.,* 1992). CRISP4, almost exclusively synthesized in the epididymis, also

associates with sperm during maturation (Jalkanen *et al.,* 2005; Nolan *et al.,* 2006, Weigel Muñoz *et al.,* 2019), inhibits Ca^{2+} channel TRPM8 (Gibbs *et al*., 2011), and participates in the fertilization process (Carvajal *et al.,* 2018; Gibbs *et al.,* 2011; Turunen *et al.,* 2012). CRISP3 exhibits a wider expression distribution including the epididymis and accessory glands within the male reproductive tract (Haendler *et al*., 1997; Schwidetzky *et al*., 1995; Udby *et al.,* 2005) as well as organs and cells with immunological functions (Reddy *et al.,* 2008). Whereas CRISP3 was found to bind to sperm with no roles in fertilization described so far (Da Ros *et al*., 2015), several reports support its association with male fertility in different species including humans (Chen *et al*., 2020; Doty *et al*., 2011; Gholami *et al.,* 2021).

In spite of clear evidence supporting the relevance of CRISP proteins for fertilization, knockout (KO) male mice for each individual CRISP remain fertile (Brukman *et al.*, 2016; Carvajal *et al.*, 2018; Da Ros *et al.,* 2008; Gibbs *et al.,* 2011; Turunen *et al.*, 2012; Volpert e*t al*., 2020; Weigel Muñoz *et al*., 2018), suggesting the existence of compensatory mechanisms among homologous CRISP family members. This idea was later confirmed by experiments from our group showing that simultaneous modifications in more than one CRISP gene can significantly impair male fertility (Curci *et al.,* 2020). Whereas males lacking epididymal CRISP1 and CRISP4 (C1/C4 DKO) were subfertile due to a significant decrease in *in vivo* fertilization (Carvajal *et al.,* 2018), males lacking CRISP1 and CRISP3 (C1/C3 DKO) were subfertile but exhibit normal *in vivo* fertilization, (Curci *et al.,* 2020), supporting the notion that fertility inhibition in this colony resulted as a consequence of post-fertilization defects. Interestingly, subfertility in *Crisp1-/-Crisp3-/-* colony was associated with a failure of *in vivo* fertilized eggs to reach the blastocyst stage, revealing the potential relevance of CRISP1 and CRISP3 for early embryo development (Curci *et al.,* 2020). Moreover, examination of ejaculated sperm within the uterus of control mated females showed that while control sperm were freely moving in the uterine fluid, *Crisp1-/-Crisp3-/-* sperm were mostly immotile and trapped into aggregates within a viscous uterine fluid (Curci *et al.,* 2020), suggesting the relevance of these two proteins for sperm survival within the female reproductive tract. Considering the expression of CRISP1 and CRISP3 in the male reproductive tract, it is possible that defects during and/or following epididymal passage are responsible for the early embryo development defects observed for the mutant males. In view of this, in the present work, we explored possible mechanisms leading to *Crisp1-/-Crisp3-/-* male phenotype and provide novel evidence supporting the contribution of the epididymis and the relevance of both CRISP1 and CRISP3 for sperm DNA integrity and early embryo development.

Results

Embryo development defects associated with the lack of CRISP1 and CRISP3 are not due to a delayed fertilization

To analyze whether defects in early embryo development were specifically linked to mutations in C*risp1* and *Crisp3* genes or could also be contributing to the subfertility of C1/C4 DKO males (Carvajal *et al.*, 2018), superovulated females were mated with mutant or control males from each DKO colony and those eggs recovered from the ampulla and reaching the two-cell stage *in vitro* (i.e. fertilized eggs) were further incubated to analyze the percentage progressing to blastocysts. Results revealed that whereas two-cell embryos from the C1/C3 DKO group showed a significant decrease in the percentage of blastocysts, those corresponding to C1/C4 DKO mice showed no differences in the percentage of blastocyst compared to controls (Table 1), supporting that early embryo development defects were caused by the simultaneous mutations of *Crisp1* and *Crisp3* genes.

Considering that delays in the time of *in vivo* fertilization could lead to embryonic development defects (Brackett *et al*., 1978; Lacham-Kaplan and Trounson, 1991, 1994; Orgebin-Crist, 1968; Orgebin-Crist and Jahad, 1977), and given the presence of aggregates of immotile sperm in the uterus of females mated with C1/C3 DKO males (Curci *et al.,* 2020), we next investigated whether the early embryo development failure in this colony was due to a delayed fertilization caused by an impaired sperm transport within the female reproductive tract. To this aim, we analyzed both sperm migration within the oviduct and *in vivo* fertilization shortly after mating (i.e 4hs) as a way to avoid the possibility that the prolonged stay of sperm within the female tract corresponding to the conventional mating schedule (18 hs), could be giving defective sperm enough time to reach the ampulla and fertilize the eggs. Using Acrosine-GFP (Green Fluorescent Protein)-tagged C1/C3 DKO or control males, we first examined sperm migration within the oviduct via fluorescence microscopy 4 hs after observation of copulatory plugs. Results indicated that both mutant and control sperm exhibited no difficulties to pass the uterotubal junction and migrate within the oviduct as judged by the presence of labeled sperm in both the lower and middle isthmus (Figure 1). The observation of very few fluorescent mutant or control sperm beyond the isthmus (Figure 1B, C) is due to the reported loss of the acrosome in sperm after reaching the middle/upper isthmus (La Spina *et al*., 2016; Muro *et al*., 2016). Consistent with these observations, examination of fertilization in the ampulla 4 hs after mating showed no significant differences between groups in the percentage of eggs recovered from the ampulla that develop to two-cell embryos *in vitro* (Figure 2A), confirming no defects in the time of arrival of sperm to the ampulla. However, once again, the eggs fertilized by mutant sperm exhibited clear defects to reach the blastocyst stage *in vitro* compared to controls (Figure 2B). Together, our observations suggest that factors other than a delayed fertilization due to transport defects were responsible for the observed embryo development phenotype of the mutant colony.

Mutant epididymal sperm already carry defects leading to embryo development failure

Given that our results had been obtained by natural mating, we next investigated whether the embryo developmental defects observed for C1/C3 DKO males appear during or after epididymal transit. To

address this question, we inseminated C1/C3 DKO mature cauda epididymal sperm into one uterine horn and control cauda sperm in the contralateral horn of superovulated females, and then analyzed the percentage of eggs recovered from the ampulla capable of reaching the two-cell and blastocyst stages *in vitro*. Results showed that although no differences between groups were observed in the percentage of two-cell embryos (Figure 2C), the percentage of two-cell embryos progressing to blastocysts was significantly lower for mutant than for control sperm (Figure 2D), revealing that sperm defects contributing to embryo development deficiencies in C1/C3 DKO males were already present at the epididymal level.

It is known that fertilization under *in vitro* conditions provides a controlled environment for gamete interaction, avoiding potential sperm selection mechanisms or delays in sperm arrival to the egg that may occur *in vivo*, and allowing a more precise analysis of the kinetics of both fertilization and embryo development. In view of this, we next conducted a series of *in vitro* fertilization (IVF) studies using capacitated epididymal sperm and eggs surrounded or devoid of their coats. Results showed that whereas no differences in either fresh or capacitated sperm were found in sperm count, viability and progressive motility between groups (Supp Table 1), co-incubation of cumulus-oocyte complexes (COC) with mutant sperm led to significantly lower percentages of both fertilized eggs evaluated by Hoechst staining (i.e. decondensing heads or two pronuclei within the ooplasm) (Figure 3A) and eggs capable of progressing to two-cell embryos (Figure 3B). Interestingly, besides these fertilization defects, when two-cell embryos continued their incubation *in vitro* and the percentage of embryos at different stages of development was analyzed, a significant decrease in the percentage of embryos reaching the morula and blastocyst stages was observed for the mutant group (Figure 3C), confirming that defects leading to embryo development failure were already present in epididymal cells and could be detected even outside the female tract environment.

To investigate whether difficulties in penetration of the egg coats that surround the egg could generate a potential delay in fertilization that finally leads to embryo development failure, *in vitro* fertilization assays were carried out using eggs devoid of both cumulus cells and ZP, and the percentage of fertilized ZP-free eggs analyzed. Under these conditions, there was a lower but still significant decrease in the percentage of eggs fertilized by mutant sperm accompanied again by significantly lower rates of blastocysts (Figure 3D, E), indicating that defects in egg coat penetration were not responsible for embryo development failure.

To further analyze the mechanisms leading to embryo development defects, ZP-free eggs were co-incubated with capacitated sperm as above and both sperm and egg DNA status within the ooplasma of fertilized eggs were analyzed by Hoechst staining. Of note, results showed that whereas all eggs with decondensing heads had already extruded the 2nd polar body in controls, in 4 out of 6 experiments, a proportion of eggs with decondensing heads corresponding to the mutant group were

still at Metaphase II (Met II) (Figure 3F), revealing defects in epididymal sperm affecting early post-fertilization events as the potential cause of the phenotype observed in the mutant colony.

Mutant epididymal sperm exhibited higher levels of both DNA fragmentation and intracellular Ca^{2+}

The finding that a proportion of eggs fertilized by epididymal mutant sperm *in vitro* were still at Met II, opened the possibility of defects in the meiotic resumption event that occurs during egg activation. Based on this, we next monitored the characteristic repetitive series of changes in intracellular Ca^{2+} concentration (Ca^{2+} oscillations) known to underpin release from meiotic arrest during egg activation and initiation of embryo development in mammalian eggs (Miyazaki *et al.*, 2006, Wakai *et al.*, 2019). For this purpose, ZP-free eggs were stained with Fluo-4 AM, co-incubated *in vitro* with control or mutant capacitated epididymal sperm and subjected to live confocal fluorescence imaging. Results showed no differences between the two genotypes in either the pattern of Ca^{2+} oscillations (Figure 4A) nor in a series of associated parameters such as the number of oscillations within 90 minutes, time until first oscillation (considered the time to gamete fusion), oscillation frequency, first transient area or first transient duration (Figure 4B-F). Together, these observations indicate that the presence of eggs still at Met II among those fertilized by mutant sperm was not due to defects in Ca^{2+} dynamics known to be critical for meiotic resumption during egg activation.

Considering that delays in early embryo development may result from the time taken by the egg to repair damaged paternal DNA (Esbert *et al*., 2018; Newman *et al.*, 2022, Nguyen *et al*., 2023), we next decided to analyze possible defects in DNA integrity in mutant cauda epididymal sperm. These studies were carried out using the sperm chromatin dispersion assay (SCD) which is based on the principle that sperm with fragmented DNA fail to produce the characteristic halo of dispersed DNA loops observed in sperm with non-fragmented DNA (Fernández *et al*., 2003). Interestingly, results showed a significantly higher level of DNA fragmentation in mutant than control sperm as indicated by the distribution of individual cells as a function of their DNA halo area and the percentage of cells failing to produce the halo (Figure 5A). To investigate whether the higher DNA fragmentation levels observed in mutant cauda sperm appear during epididymal transit, DNA fragmentation was also analyzed in immature sperm recovered from the caput region using cauda sperm from the same epididymis as control. Results showed that caput cells exhibited no differences in DNA fragmentation levels between groups, indicating that defects in DNA integrity in mutant sperm develop within the epididymis (Figure 5B). Given the well-established relationship between DNA fragmentation and oxidative stress, we next analyzed reactive oxygen species (ROS) levels in cauda epididymal sperm from control and mutant mice. Interestingly, results showed that ROS levels in mutant sperm were not higher than those observed in the control group (Figure 5C), not favoring the idea that higher sperm

DNA fragmentation levels were due to an increase in oxidative stress in mutant cells.

To assess the impact of the epididymal environment on sperm DNA fragmentation, WT cauda epididymal sperm were exposed to epididymal fluid recovered from mutant mice, and sperm DNA integrity analyzed by the SCD assay. Results showed that, under these conditions, WT sperm exhibited significantly higher levels of DNA fragmentation, supporting the relevance of epididymal fluid for sperm DNA integrity. Exposure of mutant sperm to epididymal fluid from WT mice, on the other hand, did not modify the higher DNA fragmentation levels exhibited by mutant cells (Figure 6A). Considering both reports showing that sperm DNA fragmentation can be induced by divalent cations in the presence of epididymal fluids (Gawecka *et al*., 2015; Shaman *et al.*, 2006), and that CRISP proteins are Ca^{2+} channel regulators (Ernesto *et al.*, 2015; Gibbs *et al.*, 2006; Gibbs *et al.*, 2011), we next analyzed the possibility that higher Ca^{2+} levels in the epididymis might contribute to the impaired DNA integrity of mutant sperm. For this purpose, WT cauda epididymal sperm were incubated *in vitro* with WT epididymal fluid in the presence of Ca^{2+} (10 mM), detecting significantly higher levels of DNA fragmentation in these cells compared to controls incubated in the absence of the cation (Figure 6A). As another approach to explore the involvement of Ca^{2+} in sperm DNA fragmentation, we next analyzed intracellular Ca^{2+} in cauda epididymal sperm by flow cytometry detecting significantly higher Ca^{2+} levels in mutant than control sperm either before or after capacitation (Figure 6B). Together, these observations support a dysregulation of Ca^{2+} within the epididymis and sperm as the main responsible for the higher sperm DNA fragmentation levels and, thus, the subsequent embryo development failure observed for mutant males.

Discussion

Substantial evidence supports the involvement of the epididymis in the acquisition of sperm fertilizing ability (Björkgren and Sipilä, 2019). However, limited information exists on the contribution of epididymal transit to the early stages of embryo development known to be crucial in determining the overall fitness of the organism. In this regard, whereas the molecular mechanisms underlying the impact of paternal factors on embryo development remain to be fully elucidated, the present work provides novel findings supporting the contribution of the epididymis to early embryo development and identifying CRISP1 and CRISP3 proteins as novel male factors relevant to this process.

Previous observations from our laboratory (Curci et al, 2020) showed that females mated with males with mutations in *Crisp1* and *Crisp3* genes (C1/C3 DKO) exhibited normal *in vivo* fertilization rates but significantly lower percentages of embryo development, supporting the notion that male-derived factors are required to allow for correct development of the embryo (Vallet-Buisan *et al.*, 2023). Moreover, we observed that triple knockouts lacking CRISP1, CRISP2 and CRISP3 as well quadruple

knockouts lacking the four members of the family exhibited both fertilization and embryo development defects, supporting the lack of CRISP1 and CRISP3 as relevant for the embryo development phenotype. Expanding on those observations, in the present study we confirmed an association between embryo development failure and mutations in *Crisp1* and *Crisp3* as indicated by the finding that eggs fertilized by sperm from *Crisp1*-/-*Crisp4*-/- males did not exhibit evidence of embryo development failure. Thus, whereas males from both double knockout colonies are subfertile and share the lack of CRISP1, the mechanisms underlying their subfertility are different depending on the other simultaneously deleted protein, providing information on the different functional modules that operate within the CRISP family (Curci *et al.*, 2020, Gonzalez et al, 2021), and establishing two models that uncouple fertilization from early embryo development. In this way, whereas C1/C4 DKO mice exclusively exhibiting defects in fertilization contribute to a better understanding of the mechanisms involved in gamete interaction, C1/C3 DKO males showing only defects in egg progression to blastocysts become an excellent model for elucidating the molecular mechanisms inherent to the early embryo development process.

Our findings showing the presence of aggregates of immotile sperm within the uterus of females mated with C1/C3 DKO males (Curci *et al.*, 2020) opened the possibility that a delayed fertilization due to a retarded arrival of sperm to the ampulla (the site of fertilization) could be the reason for embryo development failure as previously reported for immature sperm (Brackett *et al.*, 1978; Lacham-Kaplan and Trounson, 1991; 1994; Orgebin-Crist, 1968; Orgebin-Crist and Jahad, 1977). Evaluation of sperm migration within the female tract shortly after mating to avoid a delayed fertilization showed, however, that mutant sperm could pass through the uterotubal junction and reach the lower/middle isthmus just like control sperm, indicating that embryo development failure in mutant mice is unlikely to be due to defects in sperm transport from the uterus to the oviduct and/ or migration within the oviduct. Moreover, although the loss of the acrosomes due the occurrence of the acrosome reaction in the isthmus (La Spina *et al.*, 2016; Muro *et al.*, 2016) did not allow the detection of labeled sperm within the ampulla, our results indicated that the time of sperm arrival to the ampulla was comparable to that of control sperm as evidenced by fertilization rates not different from controls at 4 hs post copulation. However, in spite of the lack of differences in sperm arrival to the ampulla and fertilization rates observed shortly after mating, the fertilized eggs still exhibited an impaired ability to reach the blastocyst stage, not favoring the idea that a delayed fertilization and/or a consequently compromised oocyte quality could be responsible for the early embryo development defects observed in the mutant colony.

Considering various reports showing that male accessory glands contribute to proper embryo development without affecting fertilization rates (Jodar, 2019; Ma *et al.*, 2022; Vallet-Buisan *et al.*, 2023; W. S. *et al.*,1988), the possibility existed that the sperm defects leading to the embryo development phenotype were associated with the lack of CRISP1 and CRISP3 in the accessory gland

secretions. Interestingly, however, when epididymal sperm were directly inseminated into the uterus, we observed again normal fertilization rates in the ampulla accompanied by impaired embryo development, revealing that defects were already present in epididymal sperm. This conclusion was further supported by IVF studies showing that cumulus oocyte complexes fertilized by mutant epididymal sperm also exhibited embryo developmental defects. Unlike *in vivo assays*, however, IVF studies revealed fertilization defects in mutant sperm not detected by mating. This difference is likely due to the effective mechanism of sperm selection within the female reproductive tract that allows only high-quality sperm to reach the eggs (Cummins and Yanagimachi 1982) even in males with reproductive deficiencies, thus, masking sperm defects detected under *in vitro* conditions (Brukman *et al*., 2016). Nevertheless, the finding that C1/C3 DKO sperm exhibit *in vitro* fertilization capabilities similar to those reported for sperm lacking only CRISP1 (Da Ros *et al.*, 2008), does not support a major role for murine CRISP3 in gamete interaction in agreement with our previous observations for human CRISP3 (Da Ros *et al*., 2015).

The observation that ZP-free oocytes fertilized *in vitro* by mutant epididymal sperm also exhibited a lower ability to reach the blastocyst stage excluded potential delays generated by deficiencies in egg coat penetration as a cause of embryo development failure, indicating the existence of defects other than those associated with gamete interaction *per se* as responsible for the mutant colony phenotype. Interestingly, a proportion of ZP-free eggs fertilized by mutant sperm were still at Met II in contrast to all eggs exhibiting 2nd polar body in controls, supporting that immediate post-fertilization timing defects could be contributing to embryo development failure. In this regard, incorporation of the time lapse technology in human IVF treatments has highlighted the relevance of the timing of post-fertilization events and early cleavage as robust predictors of both embryo development to blastocyst and implantation success (Basile *et al*., 2015, Esbert *et al*., 2018; Meseguer *et al.*, 2011).

Our observations showing defects in meiotic resumption in eggs fertilized by mutant sperm opened the possibility that an impaired egg activation could be the cause of embryo development failure. In this regard, the well-established significance of egg Ca^{2+} oscillations in predicting the developmental competence of mouse zygotes and their pivotal role in meiosis resumption (Miyazaki *et al.*, 2006, Wakai *et al*., 2019), led us to analyze egg Ca^{2+} oscillations following fertilization by mutant sperm. Results showing no difference in the pattern of oscillations nor in the time to the first peak which is indicative of gamete fusion confirmed immediate post-fertilization defects as responsible for egg development failure, dismissing alterations in Ca^{2+} oscillations as the cause of embryo development impairment in the mutant mice.

Evidence showing that time is needed before the first embryonic cell division for activation of the egg DNA repairing machinery (Martin *et al*., 2019; Newman *et al*., 2022) together with the known association between high levels of DNA fragmentation and abnormal embryonic development

(Marinaro *et al*., 2023; Nguyen *et al*., 2023; Simon *et al*., 2014), raised the possibility that meiotic resumption failure may result from defects in sperm DNA integrity. In this regard, as spermatozoa harboring DNA damage have no mechanism for its repair but retain their ability to negotiate the female reproductive tract, reach the site of fertilization and fertilize oocytes, DNA-repairing activity relies on the oocyte once fertilization takes place (González Marin *et al*., 2012, Martin *et al*., 2019), representing a critical step in the generation of viable embryos. Our findings showing significantly higher levels of DNA fragmentation in mutant than control cauda epididymal sperm support sperm DNA damage as the potential cause of the early post-fertilization defects. In agreement with this conclusion, several embryo kinetics studies showed a significant delay in the early stage of second polar body extrusion in human eggs fertilized by sperm with DNA fragmentation (Casanovas *et al*., 2019; Esbert *et al.*, 2018; Wdowiak *et al*., 2015). Together, our observations underscore the intricate relationship between sperm DNA integrity and the regulatory role of CRISP proteins in shaping early embryonic outcomes.

How the lack of male CRISP1 and CRISP3 proteins could lead to higher levels of sperm DNA fragmentation? The finding that defects leading to embryo development in the mutant colony were present in epididymal sperm and that neither CRISP1 nor CRISP3 are expressed in the testes, supports the appearance of mutant sperm DNA fragmentation within the epididymis. In this regard, detection of these defects in cauda but not caput sperm supports that DNA integrity defects develop during epididymal transit and/or storage in agreement with the idea that the main pathways leading to DNA damage are triggered during epididymal transit (Okada *et al*., 2020; Sakkas *et al.*, 2010; Suganuma *et al.*, 2005), probably to allow elimination of defective sperm (Gawecka *et al*., 2015). Based on this, we can speculate that the lack of CRISP1 and CRISP3 in the epididymis renders sperm more susceptible to DNA degradation i.e., by reactive oxygen species. However, in spite of the commonly accepted association between DNA fragmentation and oxidative stress, our results did not show higher levels of ROS in mutant sperm, not favoring oxidative stress as the mechanism underlying DNA fragmentation in our mutant colony. These results differ from those reported for mice lacking epididymal antioxidant GPX5 (Glutathione Peroxidase 5) which showed higher incidence of embryo development and increased sperm DNA fragmentation but accompanied by higher levels of ROS in mutant sperm (Chabory *et al.,* 2009). Nevertheless, as these mice also exhibited changes in small RNAs within the epididymis (Chu *et al.*, 2020), we do not exclude the possibility that the lack of CRISP1 and CRISP3 in the epididymis may also affect the profile of small RNAs known to change during epididymal transit and to be important for embryonic development (Yuan *et al.,* 2016).

Previous reports showing induction of DNA fragmentation by exposure of mouse sperm to divalent cations (Ca^{2+} and Mn^{2+}) in the presence of luminal fluids concluded that DNA fragmentation is largely controlled by the luminal fluids with a contribution from sperm that is acquired during maturation (Gawecka *et al.*, 2015, Shaman *et al.*, 2006). This, together with the fact that all CRISP are Ca^{2+} channel regulators, opened the possibility that changes in Ca^{2+} regulation within the epididymis could

be responsible for the higher fragmentation levels observed in our mutant sperm. Consistent with this idea, our results showed a significant increase in DNA fragmentation when WT sperm were exposed to either mutant epididymal fluid or WT epididymal fluid in the presence of Ca^{2+}. These observations, together with the higher intracellular Ca^{2+} levels detected in mutant sperm, support a dysregulation in Ca^{2+} homeostasis in the epididymis as the main responsible for the observed sperm DNA integrity defects, probably through the activation of Ca^{2+}-dependent nucleases present within the epididymal fluid and/or sperm cells (Shaman *et al.*, 2006, Sotolongo *et al.*, 2005, Boaz *et al.*, 2008, Dominguez and Ward, 2009).

In summary, our observations provide strong evidence supporting the contribution of the epididymis beyond the acquisition of sperm fertilizing ability, identifying CRISP1 and CRISP3 as novel male factors relevant for sperm DNA integrity and early embryo development. Moreover, to our knowledge, this is the first report showing the relevance of epididymal proteins for early post-fertilization events. Given the existence of homologous human CRISP proteins in the epididymis and sperm playing equivalent roles to their rodent counterparts (Curci *et al.*, 2020, Gonzalez *et al.*, 2021), it is possible that CRISP are also involved in human embryogenesis through similar mechanisms. Considering the incidence of sperm DNA fragmentation in male infertility (Agarwal *et al*., 2020; Esteves *et al*., 2020), we believe our findings not only provide key information on the impact of epididymal factors on mammalian embryo development but will also contribute to a better understanding, diagnosis and treatment of human infertility.

Materials and Methods

Animals and ethical approval

Adult males (3-5 months old) from *Crisp1-/-Crisp3-/-* (Curci *et al*., 2020) or *Crisp1-/-Crisp4-/-* colonies (Carvajal, *et al.,* 2018) and control young (3-5 weeks old) or adult (2-5 months old) females were used. Animals were maintained with food and water *ad libitum* in a temperature-controlled room with a 12:12-h light:dark cycle. Approval for the study protocol was obtained from the IACUC of the Institute of Biology and Experimental Medicine (protocol N° 26/2018). All protocols were conducted in accordance with the Guide for Care and Use of Laboratory Animals published by the National Institutes of Health (NIH).

In vivo fertilization assays and in vitro embryo development

Males were caged individually for one night with superovulated females. For ovulation induction, females were treated with an i.p. injection of equine chorionic gonadotropin (5 UI, Zoetis, Buenos Aires, Argentina), followed by an i.p. injection of human chorionic gonadotropin (hCG; 5 IU, Zoetis, Buenos Aires, Argentina) 48 hours later. Mating was evaluated the following morning and considered

successful by the presence of copulatory plugs. Eggs were then recovered from the oviducts, placed in KSOM médium (Erbach *et al.*, 1994) supplemented with 0.1% (w/v) of bovine serum albumin (BSA), covered with paraffin oil (Ewe, Sanitas SA, Buenos Aires, Argentina), and incubated overnight at 37°C in an atmosphere of 5% (v/v) CO_2 in air. Eggs were considered fertilized when they reached the two-cell embryo stage. For evaluation of their development to blastocyst, two-cell embryos were incubated for an additional 3 days under the same conditions.

Sperm transport and migration within the female tract

Male mice expressing a transgene for an acrosomal EGFP were mated with superovulated females to detect sperm within the oviduct, as previously described (La Spina *et al.,* 2016; Curci *et al*., 2020). Briefly, a wild-type female subjected to superovulation was caged for 45 minutes with a transgenic male 12 hours after hCG administration. After 4 hours of detection of copulatory plug, the uterus and the oviducts were placed in KSOM medium supplemented with 0.3% (w/v) of BSA, mounted on slides, covered with coverslips and immediately observed under an Olympus IX83 microscope (Olympus Corp., Tokyo, Japan) at ×40. The number of fluorescent sperm within the oviduct was evaluated subjectively.

Epididymal sperm collection and in vitro capacitation

Mouse sperm were recovered by incising the cauda epididymis in 150 µl of capacitation medium (Fraser and Drury, 1975; Giaccagli *et al.*, 2021) supplemented with 0.3% (w/v) bovine serum albumin (BSA), pH: 7.3–7.5, allowing motile sperm to swim-out of the cauda for 10 minutes at 37°C in an atmosphere of 5% (v/v) CO_2 in air. For *in vitro* capacitation, aliquots of the swim-out suspension were added to 300 µl of capacitation medium to a final concentration of 1–10 × 10^6 spermatozoa/ml and incubated for 90 min under the same conditions.

Intrauterine insemination

For intrauterine insemination young females were superovulated as previously described. Eight hours after hCG injection, the females were anesthetized with an i.p. injection of xylazine/ketamine (10:100 mg/kg), and an incision was made in the abdomen, exposing both uterine horns. Using a syringe, 50 µl of either mutant or control swim-out sperm suspensions (1x10^7 spermatozoa/ml) were introduced into one uterine horn followed by immediate ligation, whereas the remaining sperm suspension was introduced in the contralateral horn. After approximately 15 hours, oocytes were recovered from the ampulla, placed in KSOM medium, incubated at 37°C and 5% v/v CO_2, and the percentage of cells reaching the two-cell embryo stage was analyzed the following day. Two-cell embryos were then incubated for additional 3 days under the same conditions to evaluate their development to blastocyst.

In vitro fertilization assays

Gamete interaction assays were carried out as previously reported (Curci *et al.*, 2020). Briefly, cumulus-oocyte complexes (COC) were collected from superovulated females 12-15 h after hCG administration. When needed, cumulus cells were removed by incubating the COC in 0.3 mg/ml hyaluronidase (type IV) for 3-5 min and zona pellucida (ZP) was dissolved by treating the eggs with acid Tyrode solution (pH 2.5) for 10-20 s (Nicolson *et al.*, 1975). COC were inseminated with a final concentration of 1-5 × 10^5 cells/ml and gametes were co-incubated for 3.5 h at 37°C in an atmosphere of 5% (v/v) CO_2 in air. For gamete fusion assays, ZP-free eggs were inseminated with a final concentration of 1-5 × 10^4 cells/ml and gametes co-incubated for 1 h under the same conditions. In all cases, eggs were recovered at the end of incubation, washed, fixed with 2% (w/v) paraformaldehyde in PBS and stained with 10 µg/ml Hoechst 33342 for evaluation of fertilization under epifluorescence microscope (× 200). Eggs were considered fertilized when at least one decondensing sperm nucleus or two pronuclei were observed in the egg cytoplasm. Alternatively, ZP-intact or ZP-free eggs were recovered at the end of incubation and placed in KSOM medium for 24 hs to determine the percentage reaching the two-cell embryo stage or for 3 additional days for evaluation of eggs in blastocyst stage. To avoid sticking, ZP-free eggs were incubated in individual droplets. For evaluation of progression to different stages of embryo development, two cell embryos obtained from COC were incubated for 3 days in KSOM and the percentage reaching each stage (i.e. 4/8 cells, morula or blastocyst) determined.

Analysis of sperm functional parameters

Epididymal sperm concentration was determined using a hemocytometer. Viability was assessed by staining sperm with prewarmed 0.5% (v/v) eosin Y and dye exclusion (indicative of sperm viability) analyzed under light microscopy (×400). For progressive motility assessment, sperm suspensions (15 µl) were placed between prewarmed slides and coverslips (22 mm x 22 mm) to create a chamber with 30 mm depth and sperm movement was recorded by video microscopy under a light microscope (Nikon ECLIPSE E200; Basler acA-78075gc) at 400x magnification for subsequent analysis. The percentage of progressive motile sperm was calculated by analyzing a minimum of 300 cells distributed in at least 20 different microscope fields.

Oocyte Ca^{2+} *oscillations*

ZP-free eggs were incubated with 1 µM Fluo-4 AM, 0.02% (p/v) pluronic acid and 15 µg/ml Hoechst 33342 in capacitation medium for 25 min at room temperature. Eggs were then extensively washed in fresh medium, mounted in 100 µl of medium covered with paraffin oil and analyzed on an Olympus IX83 Spinning Disk microscope (Olympus Corp., Tokyo, Japan) (x100), equipped with an

environmental chamber sustaining a temperature of 37.5 °C and 5% CO_2. Images were taken every 20 seconds. Basal Ca^{2+} was recorded for 10 minutes. Then, *in vitro* capacitated sperm were added and image recording continued for at least 1.5 hours. In all cases, fertilization was analyzed by the presence of at least one decondensing sperm head within the ooplasm. Polyspermic eggs were excluded from the analysis. Intracellular Ca^{2+} was determined in a single equatorial plane of each egg by measuring the fluorescence intensity using the ImageJ software (http://imagej.nih.gov/ij) and normalized to basal fluorescence.

Sperm chromatin dispersion (SCD) assay

Sperm DNA integrity was assessed as described before (Fernández *et al.*, 2003). Briefly, aliquots of 200 µl of sperm from swim-out in capacitating medium were mixed with 1% low-melting-point aqueous agarose (to obtain a 0.7% final agarose concentration) at 37°C. In those cases in which caput sperm were used, cells were centrifuged for 3 minutes at 1500 rpm prior to the addition of agarose. Aliquots of 50 µl of the mixture were pipetted onto a coverslip and then placed over a glass slide precoated with 0.65% standard agarose and left to solidify at 4°C for 10 minutes. Coverslips were carefully removed, and slides were immediately immersed horizontally in a tray with freshly prepared acid denaturation solution (0.08 N HCl) for 14 minutes at room temperature in the dark to generate restricted single-stranded DNA (ssDNA) motifs from DNA breaks. Then, proteins were removed by transfer of the slides to a tray with neutralizing and lysing solution 1 (0.4 M Tris, 0.8 M β-mercaptoetanol, 1% SDS, and 50 mM EDTA, pH 7.5) for 20 minutes at room temperature, which was followed by incubation in neutralizing and lysis solution 2 (0.4 M Tris, 2 M NaCl, and 1% SDS, pH 7.5) for 15 minutes at room temperature. Slides were thoroughly washed in TBE buffer (0.09 M Tris-borate and 0.002 M EDTA, pH 7.5) for 12 minutes, dehydrated in sequential 70%, 90%, and 100% ethanol baths (2 minutes each), and air dried. Cells were stained with Hoechst (10 µg/ml) in Vectashield (Vector Laboratories, Burlingame, CA) and halo surface analyzed by fluorescence microscopy on an Olympus IX83 Spinning Disk microscope (Olympus Corp., Tokyo, Japan) (x600, AN 1.42). Pictures of at least 200 sperm heads were taken and the halo area analyzed by ImageJ software (http://imagej.nih.gov/ij). Sperm DNA was considered fragmented when no halo was observed or when the halo area was smaller than twice the area corresponding to non-dispersed sperm.

Analysis of Reactive Oxygen Species (ROS)

ROS levels in sperm were measured by confocal microscopy. Briefly, after swim-out in capacitating medium without BSA, Hoechst 33342 (40 µg/ml) and CellROX-Gren (25 µM) were added and sperm incubated under these conditions for 30 minutes at 37 ºC and 5% CO_2. Samples were then fixed with 4% paraformaldehyde for 10 minutes, exposed to 100mM ammonium acetate (pH:9.0), centrifuged

at 3000 rpm for 3 minutes two times and, finally, placed over a glass slide, mounted with glycerol and analyzed on an Olympus IX83 Spinning Disk microscope (Olympus Corp., Tokyo, Japan) (x600). Images of at least 200 sperm heads for each condition were analyzed and fluorescence intensity calculated by ImageJ software (http://imagej.nih.gov/ij).

Incubation of sperm with epididymal fluids

After 10 min of swim-out in capacitating medium without BSA, sperm were centrifuged 2 min at 1500 rpm and the recovered supernatants containing diluted cauda fluid stored at 37°C in an atmosphere of 5% (v/v) CO_2 in air. Sperm were then washed two times with 1 ml of capacitating medium without BSA followed by a 2 min centrifugation at 1500 rpm. After the second centrifugation, cauda fluids from either the same or the other genotype were added and incubation continued for 1 hour at 37°C in an atmosphere of 5% (v/v) CO_2. For evaluation of the effect of Ca^{2+}, sperm were incubated as described above in the presence of 10 mM Ca^{2+} prepared from a 100X $CaCl_2$ stock solution.

Sperm Intracellular Ca^{2+} measurement

Cytoplasmic Ca^{2+} levels in sperm were measured by flow cytometry as previously described (Brukman *et al*., 2016; Curci *et al.,* 2020). Briefly, after 60 minutes of incubation in capacitation medium, sperm were loaded with 2 mM of Fluo-4 AM (Invitrogen, Carlsbad, California, USA) diluted in 10% (w/v) of Pluronic F-127 (Invitrogen) and incubated for an additional 30 minutes. Samples were washed to remove the excess of probe, resuspended in BSA-free medium, and exposed to 2.5 µg/mL of propidium iodide (PI) just before measurement. Fluorescence was detected using a BD FACSCantoTM II analyzer following the manufacturer's indications and at least 10,000 events were analyzed per sample. Data analysis was performed by FlowJo 10 software (FlowJo LLC, Ashland, OR, USA). In each condition, the fluorescence mean was normalized to basal Fluo-4-AM fluorescence.

Statistical analysis

Data represents the mean ± SEM of at least three independent experiments and “n” indicates the number of animals analyzed in each group for all experiments except for oocyte Ca^{2+} oscillations where “n” indicates the number of oocytes analyzed. Calculations were performed using the Prism 8.0 software (GraphPad Software, La Jolla, CA). Comparisons between two experimental groups were analyzed by one-way t-student test whereas comparisons among three or more groups were analyzed by two-way analysis of variance (ANOVA) followed by Fisher LSD for embryo development progression and Holm-Sidak´s for both resumption of meiosis and sperm intracellular Ca^{2+}. In those

cases in which data did not meet the assumptions required to perform two-way ANOVA (i.e. caput sperm DNA fragmentation, ROS levels and incubation with fluids), non-parametric Kruskal-Wallis followed by Dunn´s test were used. In all cases differences were considered significant at a level of $p<0.05$.

Acknowledgments

The authors would like to thank Dr Cuasnicu laboratory members, especially Dr Debora Cohen, for their helpful comments and critical input. This study was partially supported by the National Research Council of Argentina (CONICET) grant (PIP 2022) to PSC and MWM and by the National Agency for Scientific and Technological Promotion (ANPCyT) grants (PICT 2019, No 3588) to MWM and (PICT 2021. No 00765) to PSC.

Conflict of interest

The authors declare no conflicts of interest.

Author contributions

V. Sulzyk, L. Curci, M. Weigel Muñoz, and P.S. Cuasnicu designed research. V. Sulzyk, L. Curci, M. Weigel Muñoz, A. Rebagliati Cid and Gonzalez L. performed research. V. Sulzyk, M. Weigel Muñoz, and P.S. Cuasnicu analyzed data. M. Weigel Muñoz, V. Sulzyk and P.S. Cuasnicu wrote the paper.

References

Agarwal, A., Majzoub, A., Baskaran, S., Panner Selvam, M. K., Cho, C. L., Henkel, R., Finelli, R., Leisegang, K., Sengupta, P., Barbarosie, C., et al. (2020). Sperm DNA Fragmentation: A New Guideline for Clinicians. *World J. Mens. Health* 38, 412.

Basile, N., Vime, P., Florensa, M., Aparicio Ruiz, B., García Velasco, J. A., Remohí, J. and Meseguer, M. (2015). The use of morphokinetics as a predictor of implantation: a multicentric study to define and validate an algorithm for embryo selection. *Hum. Reprod.* 30, 276–283.

Björkgren, I. and Sipilä, P. (2019). The impact of epididymal proteins on sperm function. *Reproduction* 158, R155–R167.

Boaz SM, Dominguez K, Shaman JA, Ward WS. Mouse spermatozoa contain a nuclease that is activated by pretreatment with EGTA and subsequent calcium incubation. *J Cell Biochem*. 2008 Apr 1;103(5):1636-45.

Brackett, B. G., Hall, J. L. and Oh, Y. K. (1978). In vitro fertilizing ability of testicular, epididymal, and ejaculated rabbit spermatozoa. *Fertil. Steril.* 29, 571–82.

Brukman, N. G., Miyata, H., Torres, P., Lombardo, D., Caramelo, J. J., Ikawa, M., Da Ros, V. G. and Cuasnicú, P. S. (2016). Fertilization defects in sperm from Cysteine-rich secretory protein 2 (Crisp2) knockout mice: implications for fertility disorders. *Mol. Hum. Reprod.* 22, 240–51.

Busso, D., Cohen, D. J., Maldera, J. A., Dematteis, A. and Cuasnicu, P. S. (2007). A novel function for CRISP1 in rodent fertilization: involvement in sperm-zona pellucida interaction. *Biol. Reprod.* 77, 848–54.

Cameo, M. S. and Blaquier, J. A. (1976). Androgen-controlled specific proteins in rat epididymis. *J. Endocrinol.* 69, 47–55.

Carvajal, G., Brukman, N. G., Weigel Muñoz, M., Battistone, M. A., Guazzone, V. A., Ikawa, M., Haruhiko, M., Lustig, L., Breton, S. and Cuasnicu, P. S. (2018). Impaired male fertility and abnormal epididymal epithelium differentiation in mice lacking CRISP1 and CRISP4. *Sci. Rep.* 8, 17531.

Casanovas, A., Ribas-Maynou, J., Lara-Cerrillo, S., Jimenez-Macedo, A. R., Hortal, O., Benet, J., Carrera, J. and García-Peiró, A. (2019). Double-stranded sperm DNA damage is a cause of delay in embryo development and can impair implantation rates. *Fertil. Steril.* 111, 699-707.e1.

Chabory, E., Damon, C., Lenoir, A., Kauselmann, G., Kern, H., Zevnik, B., Garrel, C., Saez, F., Cadet, R., Henry-Berger, J., et al. (2009). Epididymis seleno-independent glutathione peroxidase 5 maintains sperm DNA integrity in mice. *J. Clin. Invest.119(7):2074-85.*

Chen, Y., Wei, H., Liu, Y., Gao, F., Chen, Z., Wang, P., Li, L. and Zhang, S. (2020). Identification of new protein biomarkers associated with the boar fertility using iTRAQ-based quantitative proteomic analysis. *Int. J. Biol. Macromol.* 162, 50–59.

Chu, C., Yu, L., Henry-Berger, J., Ru, Y.-F., Kocer, A., Champroux, A., Li, Z.-T., He, M., Xie, S.-S., Ma, W.-B., et al. (2020). Knockout of glutathione peroxidase 5 down-regulates the piRNAs in the caput epididymidis of aged mice. *Asian J. Androl.* 22, 590.

Cohen, D. J., Rochwerger, L., Ellerman, D. A., Morgenfeld, M. M., Busso, D. and Cuasnicú, P. S. (2000a). Relationship between the association of rat epididymal protein "DE" with spermatozoa and the behavior and function of the protein. *Mol. Reprod. Dev.* 56, 180–8.

Cohen, D. J., Ellerman, D. A. and Cuasnicú, P. S. (2000b). Mammalian sperm-egg fusion: evidence that epididymal protein DE plays a role in mouse gamete fusion. *Biol. Reprod.* 63, 462–8.

Curci, L., Brukman, N. G., Weigel Muñoz, M., Rojo, D., Carvajal, G., Sulzyk, V., Gonzalez, S. N., Rubinstein, M., Da Ros, V. G. and Cuasnicú, P. S. (2020). Functional redundancy and compensation: Deletion of multiple murine Crisp genes reveals their essential role for male fertility. *FASEB J.*

Da Ros, V. G., Maldera, J. A., Willis, W. D., Cohen, D. J., Goulding, E. H., Gelman, D. M., Rubinstein, M., Eddy, E. M. and Cuasnicu, P. S. (2008). Impaired sperm fertilizing ability in mice lacking Cysteine-RIch Secretory Protein 1 (CRISP1). *Dev. Biol.* 320, 12–18.

Da Ros, V. G., Muñoz, M. W., Battistone, M. A., Brukman, N. G., Carvajal, G., Curci, L., Gómez-Elías, M. D., Cohen, D. B. J. and Cuasnicu, P. S. (2015). From the epididymis to the egg: participation of CRISP proteins in mammalian fertilization. *Asian J. Androl.* 17, 711–5.

Doty, A., Buhi, W. C., Benson, S., Scoggin, K. E., Pozor, M., Macpherson, M., Mutz, M. and Troedsson, M. H. T. (2011). Equine CRISP3 Modulates Interaction Between Spermatozoa and Polymorphonuclear Neutrophils1. *Biol. Reprod.* 85, 157–164.

Dominguez K, Ward WS. A novel nuclease activity that is activated by Ca(2+) chelated to EGTA. Syst Biol Reprod Med. 2009 Dec;55(5-6):193-9.

Ellerman, D. A., Cohen, D. J., Da Ros, V. G., Morgenfeld, M. M., Busso, D. and Cuasnicú, P. S. (2006). Sperm protein "DE" mediates gamete fusion through an evolutionarily conserved site of the CRISP family. *Dev. Biol.* 297, 228–37.

Erbach, G. T., Lawitts, J. A., Papaioannou, V. E. and Biggers, J. D. (1994). Differential Growth of the Mouse Preimplantation Embryo in Chemically Defined Media1. *Biol. Reprod.* 50, 1027–1033.

Ernesto, J. I., Weigel Muñoz, M., Battistone, M. A., Vasen, G., Martínez-López, P., Orta, G., Figueiras-Fierro, D., De la Vega-Beltran, J. L., Moreno, I. A., Guidobaldi, H. A., et al.

(2015). CRISP1 as a novel CatSper regulator that modulates sperm motility and orientation during fertilization. *J. Cell Biol.* 210, 1213–24.

Esbert, M., Pacheco, A., Soares, S. R., Amorós, D., Florensa, M., Ballesteros, A. and Meseguer, M. (2018). High sperm DNA fragmentation delays human embryo kinetics when oocytes from young and healthy donors are microinjected. *Andrology* 6, 697–706.

Esteves, S. C., Santi, D. and Simoni, M. (2020). An update on clinical and surgical interventions to reduce sperm DNA fragmentation in infertile men. *Andrology* 8, 53–81.

Fernández, J. L., Muriel, L., Rivero, M. T., Goyanes, V., Vazquez, R. and Alvarez, J. G. (2003). The sperm chromatin dispersion test: a simple method for the determination of sperm DNA fragmentation. *J. Androl.* 24, 59–66.

Florman, H. M. and Fissore, R. A. (2015). Fertilization in Mammals. In *Knobil and Neill's Physiology of Reproduction*, pp. 149–196. Elsevier.

Fraser, L. R. and Drury, L. M. (1975). The relationship between sperm concentration and fertilization in vitro of mouse eggs. *Biol. Reprod.* 13, 513–8.

Gawecka, J. E., Boaz, S., Kasperson, K., Nguyen, H., Evenson, D. P. and Ward, W. S. (2015). Luminal fluid of epididymis and vas deferens contributes to sperm chromatin fragmentation. *Hum. Reprod.* 30(12):2725-36.

Gholami, D., Amirmahani, F., Yazdi, R. S., Hasheminia, T. and Teimori, H. (2021). MiR-182-5p, MiR-192-5p, and MiR-493-5p Constitute a Regulatory Network with CRISP3 in Seminal Plasma Fluid of Teratozoospermia Patients. *Reprod. Sci.* 28, 2060–2069.

Giaccagli, M. M., Gómez-Elías, M. D., Herzfeld, J. D., Marín-Briggiler, C. I., Cuasnicú, P. S., Cohen, D. J. and Da Ros, V. G. (2021). Capacitation-Induced Mitochondrial Activity Is Required for Sperm Fertilizing Ability in Mice by Modulating Hyperactivation. *Front. Cell Dev. Biol.* 9,.

Gibbs, G. M., Scanlon, M. J., Swarbrick, J., Curtis, S., Gallant, E., Dulhunty, A. F. and O'Bryan, M. K. (2006). The cysteine-rich secretory protein domain of Tpx-1 is related to ion channel toxins and regulates ryanodine receptor Ca2+ signaling. *J. Biol. Chem.* 281, 4156–63.

Gibbs, G. M., Roelants, K. and O'Bryan, M. K. (2008). The CAP superfamily: cysteine-rich secretory proteins, antigen 5, and pathogenesis-related 1 proteins--roles in reproduction, cancer, and immune defense. *Endocr. Rev.* 29, 865–97.

Gibbs, G. M., Orta, G., Reddy, T., Koppers, A. J., Martínez-López, P., de la Vega-Beltràn, J. L., Lo, J. C. Y., Veldhuis, N., Jamsai, D., McIntyre, P., et al. (2011). Cysteine-rich secretory protein 4 is an inhibitor of transient receptor potential M8 with a role in establishing sperm function. *Proc. Natl. Acad. Sci. U. S. A.* 108, 7034–9.

González-Marín, C., Gosálvez, J. and Roy, R. (2012). Types, Causes, Detection and Repair of DNA Fragmentation in Animal and Human Sperm Cells. *Int. J. Mol. Sci.* 13, 14026–14052.

Gonzalez, S. N., Sulzyk, V., Weigel Muñoz, M. and Cuasnicu, P. S. (2021). Cysteine-Rich Secretory Proteins (CRISP) are Key Players in Mammalian Fertilization and Fertility. *Front. Cell Dev. Biol.* 9,.

Haendler, B., Habenicht, U. F., Schwidetzky, U., Schüttke, I. and Schleuning, W. D. (1997). Differential androgen regulation of the murine genes for cysteine-rich secretory proteins (CRISP). *Eur. J. Biochem.* 250, 440–6.

Jalkanen, J., Huhtaniemi, I. and Poutanen, M. (2005). Mouse cysteine-rich secretory protein 4 (CRISP4): a member of the Crisp family exclusively expressed in the epididymis in an androgen-dependent manner. *Biol. Reprod.* 72, 1268–74.

Jodar, M. (2019). Sperm and seminal plasma RNAs: what roles do they play beyond fertilization? *Reproduction* 158, R113–R123.

La Spina, F. A., Puga Molina, L. C., Romarowski, A., Vitale, A. M., Falzone, T. L., Krapf, D., Hirohashi, N. and Buffone, M. G. (2016). Mouse sperm begin to undergo acrosomal exocytosis in the upper isthmus of the oviduct. *Dev. Biol.* 411, 172–182.

Lacham-Kaplan, O. and Trounson, A. O. (1994). Embryo development capacity of oocytes fertilized by immature sperm and sperm treated with motility stimulants. *Reprod. Fertil. Dev.* 6, 113–116.

Lacham-Kaplan, O. and Trounson, A. (1991). Fertilizing capacity of epididymal and testicular spermatozoa microinjected under the zona pellucida of the mouse oocyte. *Mol. Reprod. Dev.* 29, 85–93.

Ma, Y., Wang, J., Qiao, F. and Wang, Y. (2022). Extracellular vesicles from seminal plasma improved development of *in vitro* -fertilized mouse embryos. *Zygote* 30, 619–624.

Maeda, T., Sakashita, M., Ohba, Y. and Nakanishi, Y. (1998). Molecular cloning of the rat Tpx-1 responsible for the interaction between spermatogenic and Sertoli cells. *Biochem. Biophys. Res. Commun.* 248, 140–6.

Marinaro, J. A. (2023). Sperm DNA fragmentation and its interaction with female factors. *Fertil. Steril.* 120, 715–719.

Martin, J. H., Aitken, R. J., Bromfield, E. G. and Nixon, B. (2019). DNA damage and repair in the female germline: contributions to ART. *Hum. Reprod. Update* 25, 180–201.

Meseguer, M., Herrero, J., Tejera, A., Hilligsoe, K. M., Ramsing, N. B. and Remohi, J. (2011). The use of morphokinetics as a predictor of embryo implantation. *Hum. Reprod.* 26, 2658–2671.

Milne, T. J., Abbenante, G., Tyndall, J. D. A., Halliday, J. and Lewis, R. J. (2003). Isolation and Characterization of a Cone Snail Protease with Homology to CRISP Proteins of the Pathogenesis-related Protein Superfamily. *J. Biol. Chem.* 278, 31105–31110.

Miyazaki, S. (2006). Thirty years of calcium signals at fertilization. *Semin. Cell Dev. Biol.* 17, 233–243.

Muro, Y., Hasuwa, H., Isotani, A., Miyata, H., Yamagata, K., Ikawa, M., Yanagimachi, R. and Okabe, M. (2016). Behavior of Mouse Spermatozoa in the Female Reproductive Tract from Soon after Mating to the Beginning of Fertilization. *Biol. Reprod.* 94, 80.

Newman, H., Catt, S., Vining, B., Vollenhoven, B. and Horta, F. (2022). DNA repair and response to sperm DNA damage in oocytes and embryos, and the potential consequences in ART: a systematic review. *Mol. Hum. Reprod.* 28.

Nguyen, H., Ribas-Maynou, J., Wu, H., Quon, B., Inouye, T., Walker, B., Langaman, C., Huang, T. T. F. and Ward, W. S. (2023). Low levels of mouse sperm chromatin fragmentation delay embryo development. *Biol. Reprod.* 109, 635–643.

Nicolson, G. L., Yanagimachi, R. and Yanagimachi, H. (1975). Ultrastructural localization of lectin-binding sites on the zonae pellucidae and plasma membranes of mammalian eggs. *J. Cell Biol.* 66, 263–74.

Nolan, M. A., Wu, L., Bang, H. J., Jelinsky, S. A., Roberts, K. P., Turner, T. T., Kopf, G. S. and Johnston, D. S. (2006). Identification of rat cysteine-rich secretory protein 4 (Crisp4) as the ortholog to human CRISP1 and mouse Crisp4. *Biol. Reprod.* 74, 984–91.

Okada, F. K., Andretta, R. R. and Spaine, D. M. (2020). One day is better than four days of ejaculatory abstinence for sperm function. *Reprod. Fertil.* 1, 1–10.

Olrichs, N. K., Mahalka, A. K., Kaloyanova, D., Kinnunen, P. K. and Bernd Helms, J. (2014). Golgi-Associated plant Pathogenesis Related protein 1 (GAPR-1) forms amyloid-like fibrils by interaction with acidic phospholipids and inhibits Aβ aggregation. *Amyloid* 21, 88–96.

Orgebin-Crist, M. C. (1968). Maturation of spermatozoa in the rabbit epididymis: delayed fertilization in does inseminated with epididymal spermatozoa. *J. Reprod. Fertil.* 16, 29–33.

Orgebin-Crist, M. C. and Jahad, N. (1977). Delayed cleavage of rabbit ova after fertilization by young epididymal spermatozoa. *Biol. Reprod.* 16, 358–62.

Ramathal, C., Reijo Pera, R. A. and Chavez, S. L. (2015). Preimplantation Embryo Development and Primordial Germ Cell Lineage Specification. In *Knobil and Neill's Physiology of Reproduction*, pp. 233–265. Elsevier.

Reddy, T., Gibbs, G. M., Merriner, D. J., Kerr, J. B. and O'Bryan, M. K. (2008). Cysteine-rich secretory proteins are not exclusively expressed in the male reproductive tract. *Dev. Dyn.* 237, 3313–3323.

Ren, D., Navarro, B., Perez, G., Jackson, A. C., Hsu, S., Shi, Q., Tilly, J. L. and Clapham, D. E. (2001). A sperm ion channel required for sperm motility and male fertility. *Nature* 413, 603–609.

Robaire, B. and Hinton, B. T. (2015). The Epididymis. In *Knobil and Neill's Physiology of Reproduction*, pp. 691–771. Elsevier.

Rochwerger, L., Cohen, D. J. and Cuasnicú, P. S. (1992). Mammalian sperm-egg fusion: the rat egg has complementary sites for a sperm protein that mediates gamete fusion. *Dev. Biol.* 153, 83–90.

Sakkas, D. and Alvarez, J. G. (2010). Sperm DNA fragmentation: mechanisms of origin, impact on reproductive outcome, and analysis. *Fertil. Steril.* 93, 1027–1036.

Schwidetzky, U., Haendler, B. and Schleuning, W. D. (1995). Isolation and characterization of the androgen-dependent mouse cysteine-rich secretory protein-3 (CRISP-3) gene. *Biochem. J.* 309 (Pt 3), 831–6.

Shaman, J. A., Prisztoka, R. and Ward, W. S. (2006). Topoisomerase IIB and an extracellular nuclease interact to digest sperm DNA in an apoptotic-like manner. *Biol. Reprod.* 75, 741–8.

Sheng, J., Olrichs, N. K., Geerts, W. J., Li, X., Rehman, A. U., Gadella, B. M., Kaloyanova, D. V. and Helms, J. B. (2019). Zinc binding regulates amyloid-like aggregation of GAPR-1. *Biosci. Rep.* 39,.

Simon, L., Murphy, K., Shamsi, M. B., Liu, L., Emery, B., Aston, K. I., Hotaling, J. and Carrell, D. T. (2014). Paternal influence of sperm DNA integrity on early embryonic development. *Hum. Reprod.* 29, 2402–2412.

Sotolongo B, Huang TT, Isenberger E, Ward WS. An endogenous nuclease in hamster, mouse, and human spermatozoa cleaves DNA into loop-sized fragments. *J Androl*. 2005 Mar-Apr;26(2):272-80.

Suganuma, R., Yanagimachi, R. and Meistrich, M. L. (2005). Decline in fertility of mouse sperm with abnormal chromatin during epididymal passage as revealed by ICSI. *Hum. Reprod.* 20, 3101–3108.

Sun, X., Zhu, Y., Wang, L., Liu, H., Ling, Y., Li, Z. and Sun, L. (2017). The Catsper channel and its roles in male fertility: a systematic review. *Reprod. Biol. Endocrinol.* 15, 65.

Turunen, H. T., Sipila, P., Krutskikh, A., Toivanen, J., Mankonen, H., Hamalainen, V., Bjorkgren, I., Huhtaniemi, I. and Poutanen, M. (2012). Loss of Cysteine-Rich Secretory Protein 4 (Crisp4) Leads to Deficiency in Sperm-Zona Pellucida Interaction in Mice. *Biol. Reprod.* 86, 1–8.

Udby, L. (2005). Characterization and Localization of Cysteine-Rich Secretory Protein 3 (CRISP-3) in the Human Male Reproductive Tract. *J. Androl.* 26, 333–342.

Vallet-Buisan, M., Mecca, R., Jones, C., Coward, K. and Yeste, M. (2023). Contribution of semen to early embryo development: fertilization and beyond. *Hum. Reprod. Update* 29, 395–433.

Volpert, M., Furic, L., Hu, J., O'Connor, A. E., Rebello, R. J., Keerthikumar, S., Evans, J., Merriner, D. J., Pedersen, J., Risbridger, G. P., et al. (2020). CRISP3 expression drives prostate cancer invasion and progression. *Endocr. Relat. Cancer* 27, 415–430.

W. S., O., Chen, H. Q. and Chow, P. H. (1988). Effects of male accessory sex gland secretions on early embryonic development in the golden hamster. *Reproduction* 84, 341–344.

Wakai, T., Mehregan, A. and Fissore, R. A. (2019). Ca^{2+} Signaling and Homeostasis in Mammalian Oocytes and Eggs. *Cold Spring Harb. Perspect. Biol.* 11, a035162.

Wdowiak, A., Bakalczuk, S. and Bakalczuk, G. (2015). The effect of sperm DNA fragmentation on the dynamics of the embryonic development in intracytoplasmatic sperm injection. *Reprod. Biol.* 15, 94–100.

Weigel Muñoz, M., Battistone, A. M., Carvajal, G., Maldera, J. A., Curci, L., Torres, P., Lombardo, D., Pignataro, O. P., Da Ros, V. G. and Cuasnicu, P. S. (2018). Influence of the genetic background on the reproductive phenotype of mice lacking Cysteine-RIch Secretory Protein 1 (CRISP1). *Biol. Reprod.*

Weigel Muñoz, M., Carvajal, G., Curci, L., Gonzalez, S. N. and Cuasnicu, P. S. (2019). Relevance of CRISP proteins for epididymal physiology, fertilization, and fertility. *Andrology*.

Yamazaki, Y., Brown, R. L. and Morita, T. (2002). Purification and cloning of toxins from elapid venoms that target cyclic nucleotide-gated ion channels. *Biochemistry* 41, 11331–7.

Yuan, S., Schuster, A., Tang, C., Yu, T., Ortogero, N., Bao, J., Zheng, H. and Yan, W. (2016). Sperm-borne miRNAs and endo-siRNAs are important for fertilization and preimplantation embryonic development. *Development* 143, 635–47.

Figure legends

FIGURE 1. Sperm migration through the female reproductive tract. **A**. Representative diagram showing sperm within the different regions of the female reproductive tract. UTJ, utero-tubal junction. Superovulated females were mated with Acrosine-GFP control or C1/C3 DKO males and, 4 hours after mating, sperm were analyzed inside the tract by fluorescence microscopy. **B.** Bright field (upper panel) and fluorescence (lower panel) images of the reproductive tract of a female mated with a control male (x40). **C.** Bright field (upper panel) and fluorescence (lower panel) images of the reproductive tract of a female mated with C1/C3 DKO male (x40). Figures are representative of at least 3 independent experiments.

FIGURE 2. *In vivo* fertilization and embryo development A. Control and C1/C3 DKO males were mated with superovulated females and the percentage of fertilized eggs recovered from the ampulla 4 hours after mating was evaluated. Eggs were considered fertilized when they reached the two-cell embryo stage 24 h after *in vitro* incubation. **B.** Two-cell embryos from **A** were incubated *in vitro* for an additional 3 days, and the percentage reaching the blastocyst stage was determined. **C.** Control or C1/C3 DKO cauda epididymal sperm were inseminated into the uterus of superovulated females. After 15 h, eggs were recovered from the ampulla, incubated for 24 hours *in vitro* and were considered

fertilized when reaching the two-cell embryo stage. **D.** Two-cell embryos from **C** were incubated *in vitro* for an additional 3 days and the percentage reaching the blastocyst stage was determined. Data are mean ± SEM; n=5, *p<0.05; **p<0.01. Percentages of two-cell embryos were determined by dividing the number of two-cell embryos by the total number of eggs examined and percentages of blastocysts as the number of eggs reaching the blastocyst stage divided by the total number of two cell embryos recovered.

FIGURE 3. *In vitro* fertilization and embryo development. A, B. *In vitro* capacitated control or C1/C3 DKO cauda epididymal sperm were co-incubated with cumulus oocyte complexes (COC) for 3.5 hs. Eggs were either analyzed at that moment and considered fertilized when at least one decondensing sperm nucleus or two pronuclei were found in the ooplasm (n=3) (**A**) or incubated for additional 24 hs to determine the percentage reaching the two-cell embryo stage (n=7) (**B**). **C.** Two-cell embryos from **B** were incubated for 3 days *in vitro* and the percentage reaching 4/8 cells (day 1), morula (day 2) or blastocyst (day 3) stages determined (n=7). **D.** *In vitro* capacitated control or C1/C3 DKO epididymal sperm were co-incubated with ZP-free eggs for 1 h and fertilization was evaluated by DNA staining. Eggs were considered fertilized when at least one decondensing sperm nucleus was found in the ooplasm (n≥5). **E.** Fertilized ZP-free eggs obtained as in D were incubated for an additional 3 days *in vitro* and the percentage progressing to blastocysts was determined. (n=5). **F.** Fertilized eggs from **D** were analyzed for maternal DNA status and classified as arrested in Metaphase II (Met II) or exhibiting 2nd polar body (2PB) (n≥5). Data are the mean ± SEM; *p< 0.05; **p < 0.01. Percentages of fertilization were determined by dividing the number of fertilized eggs by the total number of eggs examined. Percentages of two-cell embryos were determined by dividing the number of two-cell embryos by the total number of eggs examined. Percentages of either 4/8 cell embryos, morula and blastocysts were calculated as the number of embryos reaching each of these stages divided by the total number of two cell embryos obtained.

FIGURE 4: Egg Ca^{2+} oscillations in *in vitro* fertilized eggs. A. Representative traces of Ca^{2+} oscillation patterns following *in vitro* fertilization of ZP-free eggs with control or C1/C3 DKO sperm. Arrows indicate the time of sperm addition. **B.** Number of peaks within 90 minutes, **C.** Time to first peak, **D.** Oscillation frequency, **E.** First peak area under the curve and **F.** First transient duration. Values were normalized to basal Ca^{2+} levels recorded prior to sperm addition. Data are mean ± SEM of at least 9 oocytes from 3 independent experiments; A-F: ns.

FIGURE 5. Sperm DNA fragmentation and ROS levels. A. DNA fragmentation of control or C1/C3 DKO cauda epididymal sperm was analyzed by SCD assay and both the area of DNA halo in each individual cell (left panel) and the percentage of sperm heads with small or no halo (right panel) determined. **B.** DNA fragmentation of cauda and caput epididymal control or C1/C3 DKO sperm was

analyzed by SCD assay and the area of DNA halo in each individual cell determined. **C.** ROS levels in control and C1/C3 DKO cauda sperm analyzed by fluorescence confocal microscopy. Absence of probe and presence of Oligomycin were used as negative and positive controls, respectively. In all cases n=4. *p<0,05; ****p < 0,0001, Different letters indicate significant differences between treatments, p<0.0001.

FIGURE 6. Influence of epididymal fluid on sperm DNA integrity and intracellular Ca^{2+} levels. **A.** DNA fragmentation of control or C1/C3 DKO cauda epididymal sperm incubated for one hour with their own or the other genotype epididymal fluid in the presence or absence of 10mM Ca^{2+} was analyzed by SCD assay and the area of DNA halo in each individual cell determined. Different letters indicate significant differences between treatments (p<0.05). **B.** Intracellular Ca^{2+} levels were evaluated by flow cytometry using Fluo-4-AM probe. Results are shown as normalized mean fluorescence intensity (rMFI) of Fluo-4-AM compared to the control condition in each experiment for non-capacitated (fresh) and capacitated (CAP) sperm. Data are mean ± SEM, n= 5; *p<0,05.

Table 1. Analysis of embryo development corresponding to C1/C3 and C1/C4 DKO males

	Control	C1/C3 DKO	Control	C1/C4 DKO
Total two-cell embryos (N°)	53	53	80	76
Blastocysts (N°)	38	23	52	46
Embryo development (%)	75,2 ± 8,3%	37,4 ± 10,7% **	67,7 ± 12,1%	66,9 ± 13,4%

*Note: Percentage of embryo development was calculated as the mean of at least 5 independent experiments n = 5. ** p< 0.01 vs control.*

Figure 1

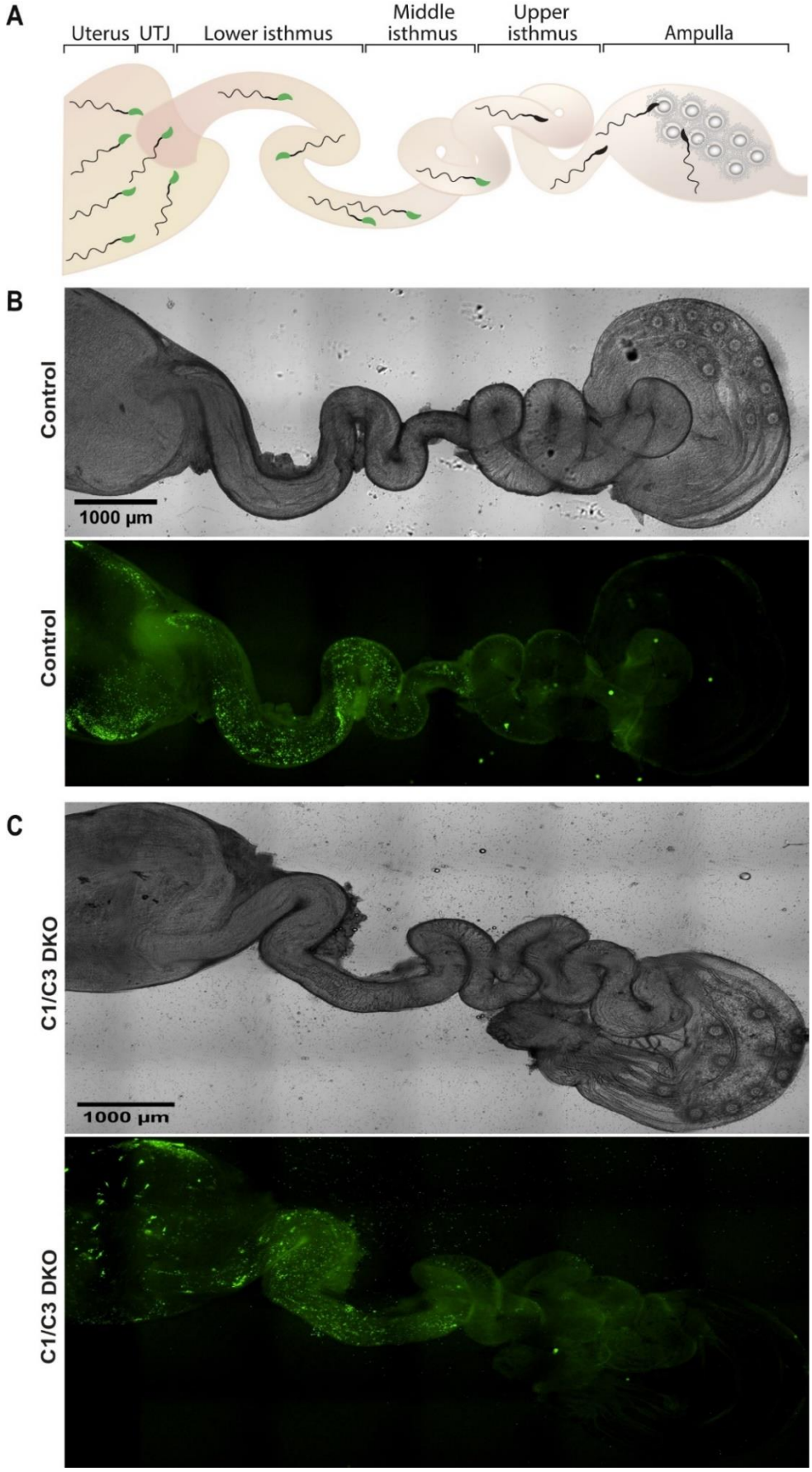
A
Uterus
UTJ
Lower isthmus
Middle isthmus
Upper isthmus
Ampulla
B
Control
1000 µm
Control
C
C1/C3 DKO
1000 µm
C1/C3 DKO

Figure 2

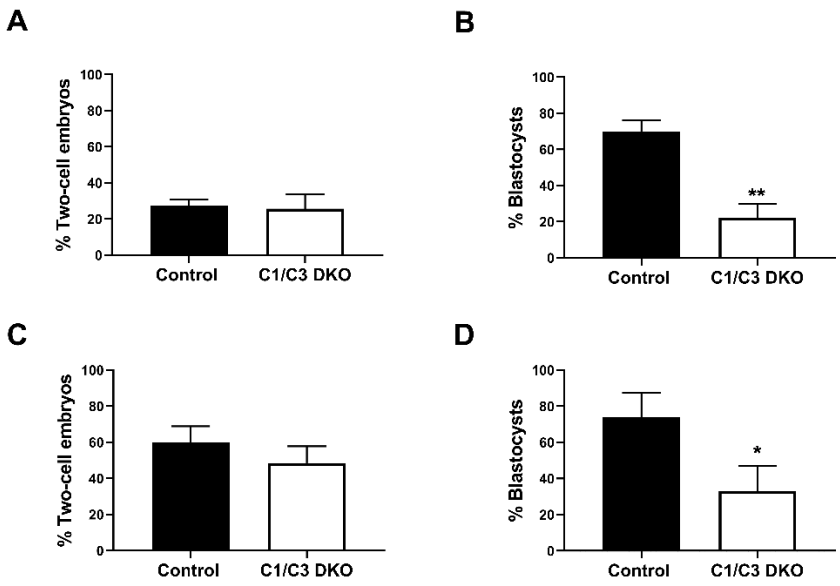
A
% Two-cell embryos
100
80
60
40
20
0
Control
C1/C3 DKO
B
% Blastocysts
100
80
60
40
20
0
**
Control
C1/C3 DKO
C
% Two-cell embryos
100
80
60
40
20
0
Control
C1/C3 DKO
D
% Blastocysts
100
80
60
40
20
0
*
Control
C1/C3 DKO

Figure 3

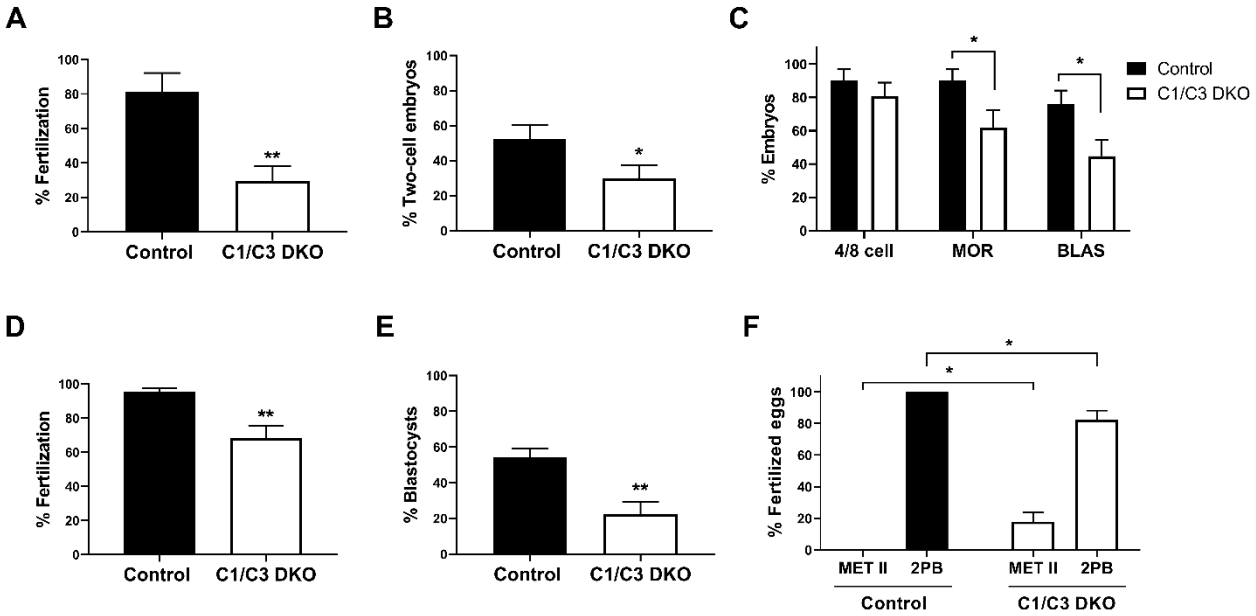
A
% Fertilization
100
80
60
40
20
0
**
Control
C1/C3 DKO
B
% Two-cell embryos
100
80
60
40
20
0
*
Control
C1/C3 DKO
C
% Embryos
100
80
60
40
20
0
*
*
Control
C1/C3 DKO
4/8 cell
MOR
BLAS
D
% Fertilization
100
80
60
40
20
0
**
Control
C1/C3 DKO
E
% Blastocysts
100
80
60
40
20
0
**
Control
C1/C3 DKO
F
% Fertilized eggs
100
80
60
40
20
0
*
*
MET II
2PB
MET II
2PB
Control
C1/C3 DKO

Figure 4

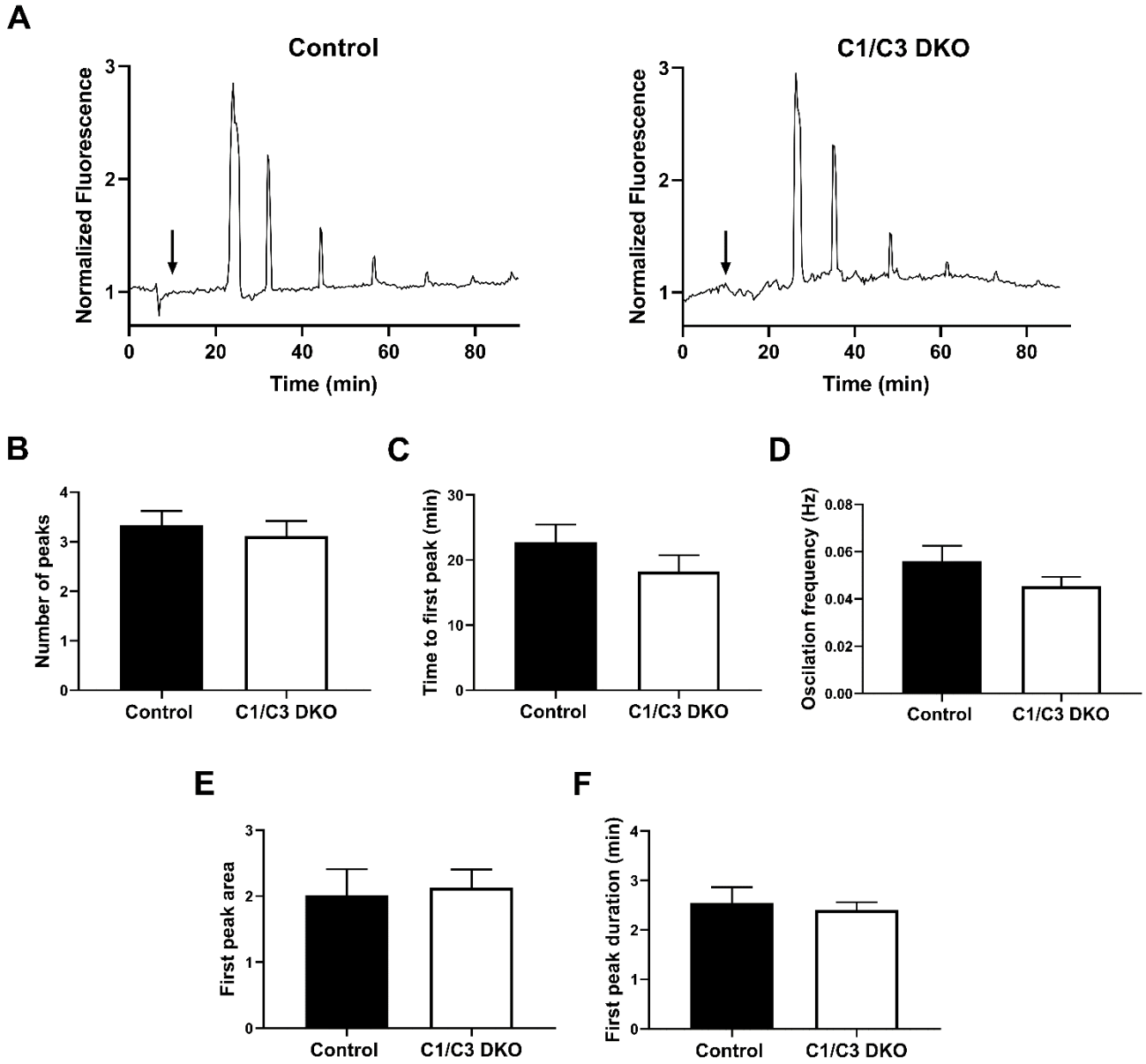
A
Control
C1/C3 DKO
Normalized Fluorescence
Time (min)
B
Number of peaks
C
Time to first peak (min)
D
Oscilation frequency (Hz)
E
First peak area
F
First peak duration (min)
Control
C1/C3 DKO

Figure 5

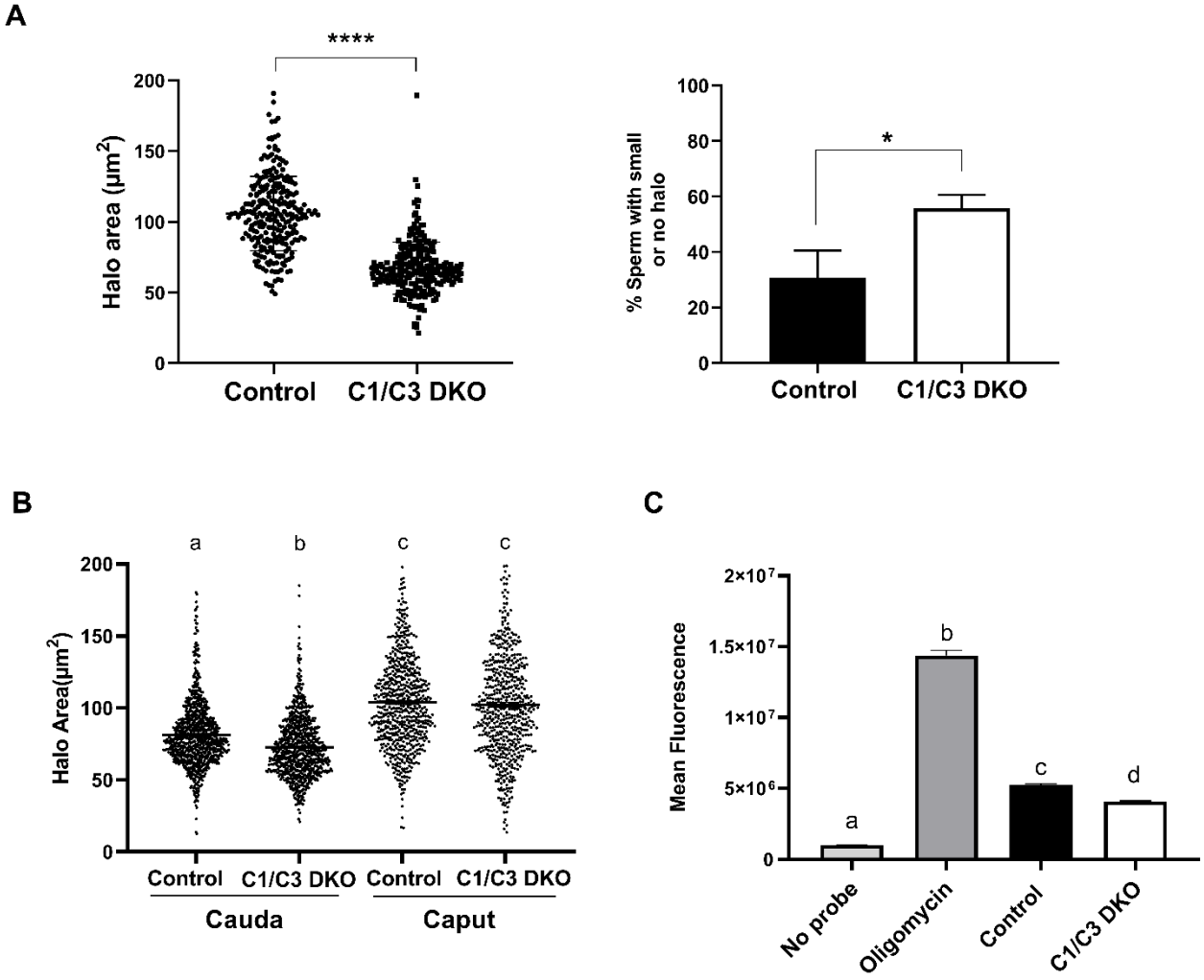
A
****
Halo area (μm²)
200
150
100
50
0
Control
C1/C3 DKO
% Sperm with small or no halo
100
80
60
40
20
0
*
Control
C1/C3 DKO
B
a
b
c
c
Halo Area(μm²)
200
150
100
50
0
Control
C1/C3 DKO
Control
C1/C3 DKO
Cauda
Caput
C
Mean Fluorescence
2×10⁷
1.5×10⁷
1×10⁷
5×10⁶
0
a
b
c
d
No probe
Oligomycin
Control
C1/C3 DKO

Figure 6

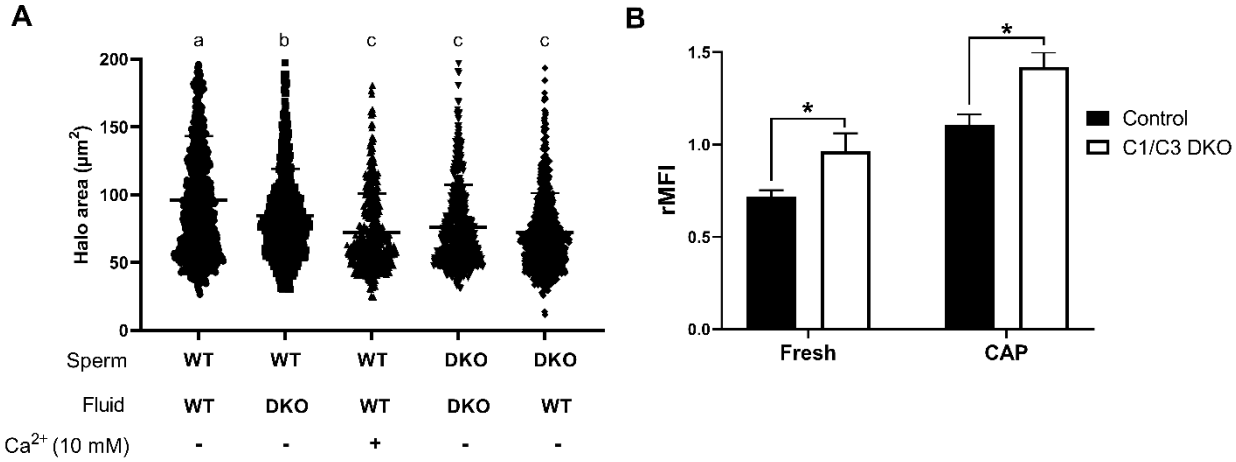
A
a
b
c
c
c
Halo area (μm²)
200
150
100
50
0
Sperm
WT
WT
WT
DKO
DKO
Fluid
WT
DKO
WT
DKO
WT
Ca²⁺ (10 mM)
-
-
+
-
-
B
rMFI
1.5
1.0
0.5
0.0
*
*
Fresh
CAP
Control
C1/C3 DKO

Table Supp. 1. Analysis of different parameters in fresh and capacitated sperm

	Control		C1/C3 DKO	
	Fresh	Capacitated	Fresh	Capacitated
Sperm count (10^6/ml)	48,35 ± 3,83	---	59,87 ± 12,03	---
Viability (%)	66,22 ± 5,25	61,04 ± 2,78	65,54 ± 2,29	58,21 ± 4,31
Progressive motility (%)	63,99 ± 1,14	57,91 ± 2,39	62,65 ± 2,37	54,27 ± 3,19

ns.